

Resistance steps in underdamped Josephson-junction arrays

Wenbin Yu and D. Stroud

Department of Physics, The Ohio State University, Columbus, Ohio 43210

(Received 29 June 1992)

The response of $N \times N$ underdamped Josephson-junction arrays to dc-current bias and dc-voltage bias is studied numerically. The current-voltage ($I - \langle V \rangle$) relation reveals a substantial hysteresis. If a dc-current bias is applied to inhomogeneous underdamped arrays (i.e., arrays with a random distribution of junction critical currents), the $I - \langle V \rangle$ curve exhibits many (but no more than N) steplike increases of resistance, in agreement with experiments of Tighe, Johnson, and Tinkham. These steps are shown to arise from row-switching behavior of the arrays, in which one or several rows of junctions across the width of the array switch simultaneously from a supercurrent state to a resistively dissipative state. If the array is voltage biased rather than current biased, this row-switching behavior is observed even in homogeneous underdamped arrays, in qualitative agreement with the experiments of van der Zant *et al.* The resistive steps persist in an applied magnetic field and melt at sufficiently high temperature. We find no evidence for row switching in overdamped arrays, whether they are current biased or voltage biased. We speculate briefly about the physical origins of this behavior.

The dynamical properties of two-dimensional Josephson-junction arrays (2D JJA's) have been extensively studied in recent years.¹⁻¹⁷ Most investigations have focused on overdamped arrays and many^{1-8,12-14} have been concerned primarily with Shapiro steps, that is, with quantized voltage plateaus which occur when a combined dc and ac current is applied. A recent calculation¹⁶ has extended these studies to underdamped arrays, and has investigated the conditions for the occurrence of chaotic dynamical states under the influence of an ac drive.

Even in the presence of a dc drive, underdamped Josephson-junction arrays sometimes exhibit a phenomenon not observed in overdamped arrays, namely, steplike increases of the resistance.¹⁸⁻²¹ These steps are thought to arise from the simultaneous switching of an entire row of junctions from a "supercurrent state" (in which the voltage drop across the row is zero) to a resistively dissipative state. They are therefore apparently associated with the hysteresis long known to occur in single underdamped junctions. Each junction in the switched row is parallel to the applied current, but the row itself is perpendicular to the direction of current flow. Thus, on any given resistance step, the voltage drop across the array is thought to be localized on several switched rows.

This article presents a calculation for both underdamped and overdamped Josephson-junction arrays, in which we numerically investigate the conditions for the observation of resistance steps. We find that resistance steps and row-switching behavior are associated only with underdamped arrays. In current-biased underdamped arrays (that is, arrays subjected to a fixed external current), the row-switching behavior is observed only in "inhomogeneous" arrays, that is, arrays with a random distribution of junction critical currents. In voltage-biased underdamped arrays, by contrast, we observe row

switching even in homogeneous arrays. In both cases, the row switching and resistance steps persist in an applied magnetic field, and the resistance steps melt if the temperature is increased sufficiently. For overdamped arrays, whether current biased or voltage biased, and whether homogeneous or inhomogeneous, we find no evidence for row switching.

Our calculations are carried out for square Josephson-junction networks. An external current or voltage is applied to the array by means of current or voltage buses (i.e., lines of constant voltage) at two opposite edges of the array. This boundary condition differs slightly from the injection method used in our previous calculations, but probably resembles more closely the typical experimental arrangement. In the transverse direction, periodic boundary conditions are usually imposed. Within the array, each superconducting grain is coupled to its four neighbors via Josephson links.

The system is described by the equations of a network of resistively and capacitively shunted Josephson junctions (the "RCSJ model"):

$$I_{ij} = C_{ij} \frac{d}{dt} V_{ij} + \frac{V_{ij}}{R_{ij}} + I_{c,ij} \sin(\phi_i - \phi_j - A_{ij}) + I_{L,ij}(t), \quad (1)$$

$$V_{ij} \equiv V_i - V_j = \frac{\hbar}{2e} \frac{d}{dt} (\phi_i - \phi_j), \quad (2)$$

$$\sum_j I_{ij} + C_{ii} \frac{d}{dt} V_i = I_{i,\text{ext}}, \quad (3)$$

$$A_{ij} = \frac{2\pi}{\Phi_0} \int_{\mathbf{x}_i}^{\mathbf{x}_j} \mathbf{A} \cdot d\mathbf{x}. \quad (4)$$

Here I_{ij} is the total current from grain i to grain j ; C_{ij} and R_{ij} are the shunt capacitance and shunt resistance between grains i and j ; C_{ii} is the capacitance between grain i and the potential ground; V_i is the voltage of grain i ; $I_{c,ij}$ is the critical current of the ij th junction; ϕ_i is the phase of grain i ; \mathbf{A} is the vector potential; $\Phi_0 = hc/2e$ is the magnetic flux quantum; \mathbf{x}_i is the position of the center of grain i ; and $I_{L,ij}(t)$ is the Langevin noise current which vanishes at zero temperature. Equation (1) expresses the total current I_{ij} from grain i to grain j as a sum of four contributions: the Ohmic current V_{ij}/R_{ij} through the shunt resistance; the charging current $C_{ij} \frac{d}{dt} V_{ij}$ through the shunt capacitance; the Josephson supercurrent; and the Langevin noise current $I_{L,ij}(t)$. Equation (2) is the Josephson relation; and Eq. (3) is Kirchhoff's Law, which expresses current conservation at each grain i . Finally, $I_{i,\text{ext}}$ is the external current injected into or extracted from each grain i : $I_{i,\text{ext}} = 0$ on an internal grain, and $I_{i,\text{ext}}$ equals the external bias current per grain on the input and output buses.

Equations (1), (2), and (3) can be combined to give

$$\begin{aligned} \sum_j \tilde{C}_{ij} \frac{d}{dt} V_j &= I_{i,\text{ext}} - \sum_j \frac{V_i - V_j}{R_{ij}} \\ &\quad - \sum_j I_{c,ij} \sin(\phi_i - \phi_j - A_{ij}) - \sum_j I_{L,ij}(t) \\ &\equiv S_i, \end{aligned} \quad (5)$$

$$\frac{d}{dt} \phi_i = \frac{2e}{\hbar} V_i, \quad (6)$$

where $\tilde{C}_{ii} = C_{ii} + \sum_{j \neq i} C_{ij}$ and $\tilde{C}_{ij} = -C_{ij}$. Equation (5) can be inverted to give

$$\frac{d}{dt} \mathbf{V} = \tilde{\mathbf{C}}^{-1} \cdot \mathbf{S}(\{V_i\}, \{\phi_i\}, t), \quad (7)$$

where \mathbf{V} and \mathbf{S} are the column vectors corresponding to the grain voltages $V_i(t)$ and the sums $S_i(t)$. The coupled equations (6) and (7) are solved by a straightforward Euler iteration, as described previously,^{3,6} with time step Δt . Δt is usually chosen as $0.04t_0$, but occasionally as small as $0.01t_0$ to $0.02t_0$, where $t_0 = \hbar/(2eRI_c)$ is the characteristic damping time. A second-order Runge-Kutta method leads to little changes in the results. In the calculations, we always start the iterations from zero-applied external current or voltage. The initial phase of each grain is independently chosen from a uniform distribution of random numbers on $(0, 2\pi)$, but the initial voltage of each grain is set equal to zero, consistent with the likely experimental conditions. When increasing or decreasing the applied bias current or voltage, we use the final phase and voltage configurations of the array at the previous bias as the initial conditions for the new bias. Usually we discard the values for the first time interval of $200t_0$ and carry out averages over the next $600t_0$ time interval (but occasionally over as long as $1000t_0$ to $1200t_0$).

In all calculations in this paper, we set all the diagonal capacitances C_{ii} equal to the same constant C_d , while the off-diagonal capacitances are taken to vanish except

for the nearest-neighbor ones, which are set equal to C_c . The Langevin noise current $I_{L,ij}(t)$ is taken to satisfy²²

$$\langle I_{L,ij}(t) \rangle = 0, \quad (8)$$

$$\langle I_{L,ij}(t) I_{L,kl}(t') \rangle = \frac{2k_B T}{R_{ij}} \delta(t - t') \delta_{ij,kl},$$

where k_B is the Boltzmann constant, T is the temperature, and $\langle \dots \rangle$ denotes the ensemble average. We have generally selected $I_{L,ij}(t)$ for each bond from a Gaussian distribution of random numbers which obeys Eq. (8).

Figure 1 shows a typical current-biased calculated $I - \langle V \rangle$ characteristic for a homogeneous array at temperature $T = 0$ and several different values of the frustration parameter $f = \Phi/\Phi_0$ (Φ is the flux through a single plaquette). In all cases shown, the diagonal McCumber-Stewart parameter²³ $\beta_d \equiv 2eC_d R^2 I_c / \hbar$ is taken as 0.1, while the off-diagonal parameter $\beta_c \equiv 2eC_c R^2 I_c / \hbar = 10$. This choice of parameters seems reasonable for some of the experimentally studied underdamped arrays, since the off-diagonal capacitance is expected to be significantly larger than the capacitance to ground.²⁴ As expected for this range of parameters, there is a noticeable hysteresis on the $I - \langle V \rangle$ characteristics,²⁵ the voltage remaining on the (upper) resistive branch when the current is decreasing. We have checked that this hysteresis is insensitive to the rate at which the current is ramped up or down and the time interval over which the voltage is averaged. The area between the two branches of the

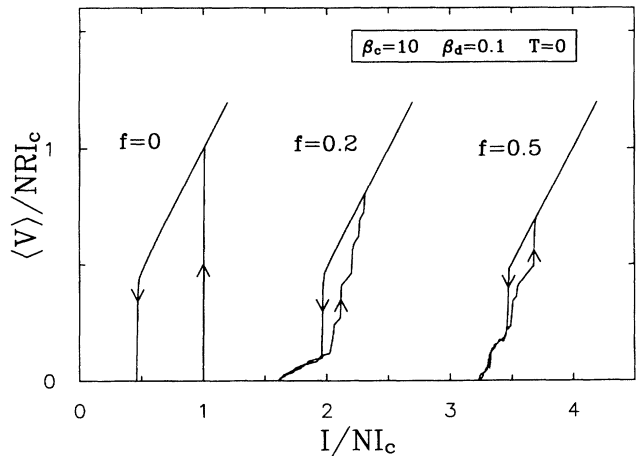


FIG. 1. Calculated time-averaged voltage drop $\langle V \rangle$ across an $N \times N$ homogeneous underdamped array ($N = 10$) as a function of dc bias current I at several values of the perpendicular magnetic flux f , assuming temperature $T = 0$ and periodic boundary conditions. The field is expressed in terms of $f = \Phi/\Phi_0$, where $\Phi_0 = hc/(2e)$ is the flux quantum, and Φ is the flux through a unit cell. The curves are offset horizontally by 1.5 units. R and I_c are the shunt resistance and critical current of each junction. β_d and β_c are the McCumber-Stewart parameters for the grain-to-ground capacitance and the intergrain capacitance. Free boundary conditions yield similar results. Arrows denote plots for increasing and decreasing current. Note that I is the total current injected into the array.

$I - \langle V \rangle$ characteristic is reduced by a magnetic field, as is the critical current.

Figure 2(a) shows the calculated $I - \langle V \rangle$ characteristics of a 10×10 inhomogeneous array at temperature $T = 0$ and various values of the frustration. The critical current on each bond $I_{c;ij}$ is taken to be a random value between $0.5I_c$ and $1.5I_c$, but the product $I_{c;ij}R_{ij}$ is assumed the same for each junction, as expected from the Ambegaokar-Baratoff expression for the critical current.²⁶ The parameters β_c and β_d are taken as the same for each junction and equal to 10 and 0.1 as in Fig. 1.

The corresponding current-resistance characteristic is shown in Fig. 2(b). In contrast to Fig. 1, there are now many steps on the current-resistance characteristic when $f = 0$, consistent with experiments.¹⁹ The steps are unevenly spaced, presumably because the shunt resistances vary from junction to junction. The number of steps

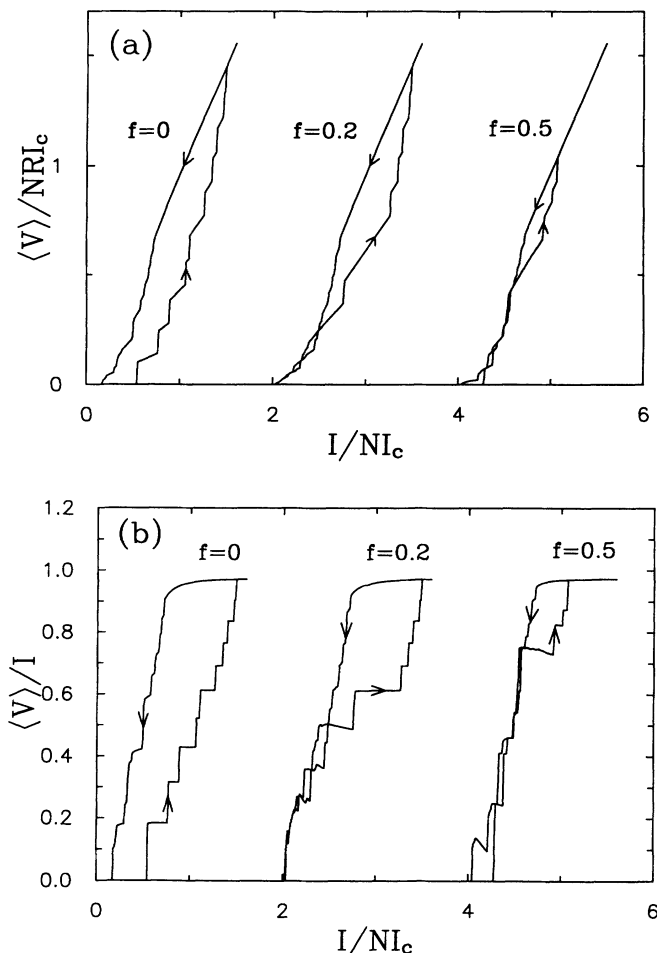


FIG. 2. (a) Same as Fig. 1 at $\beta_d = 0.1$, $\beta_c = 10$, and $T = 0$, but for an inhomogeneous array, in which the individual junction critical currents are uniformly and randomly distributed between $0.5I_c$ and $1.5I_c$. The curves are offset horizontally by two units. (b) Calculated average array resistance $\mathcal{R} \equiv \langle V \rangle / I$ (in units of R) for the curves in (a), plotted as functions of dc bias current I . The curves are offset horizontally as in (a).

never exceeds the number of rows of junctions in the array. We have calculated the time-averaged voltage of each grain in the array, as a function of external current, and have verified that the resistance steps arise from “row-switching” behavior: one or several rows of junctions across the width of the array simultaneously switch from a supercurrent state to a resistively dissipative state. The time-averaged voltage is found to be the same for each grain on a given line perpendicular to the direction of current flow. The steps persist in the presence of an applied magnetic field, as does the hysteresis (which is again insensitive to the rate at which the current is ramped up and down, and the time interval over which the voltage is averaged). These results are generally in agreement with the experimental results of Tighe *et al.*,¹⁹ who use current-driven underdamped arrays with critical current distributions probably comparable to our own.

If, instead of a current bias, we apply a voltage bias to the array, we observe “row-switching” behavior even in homogeneous arrays.¹⁸ Figure 3 shows our calculated $V - \langle I \rangle$ characteristics for an $N \times N$ voltage-biased homogeneous array ($N = 10$) at $T = 0$ and at two different values of the frustration. The corresponding voltage-resistance ($V - \mathcal{R}$) curves are shown in the insets, where $\mathcal{R} = V / \langle I \rangle$. When $f = 0$, we find 9 steps on the $V - \mathcal{R}$ curves, while exactly 10 steps appear at $f = 0.2$. As previously, the number of steps is never greater than the number of rows in the array. At $f = 0.2$ but not at $f = 0$, the steps are unevenly spaced, with resistance jumps sometimes less than the value $0.1R$ expected when a single row switches at $f = 0$.

We now speculate why row-switching behavior is observed even in homogeneous voltage-biased arrays, but only in nonhomogeneous current-biased arrays. In our homogeneous arrays, if an individual junction is sufficiently underdamped, it can have a resistance $\langle V \rangle / I = 0$ or R , depending on which branch of the $I - \langle V \rangle$ charac-

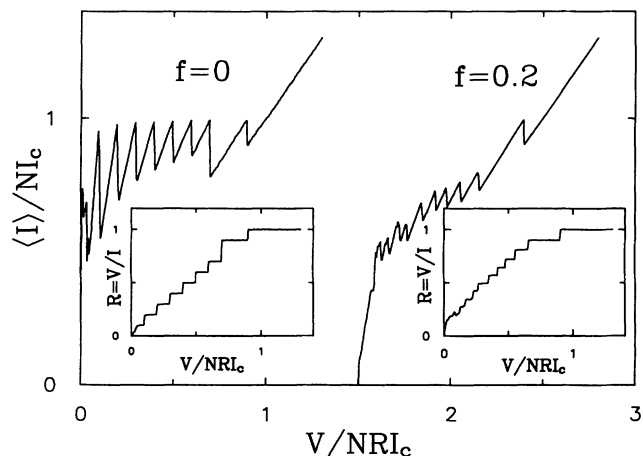


FIG. 3. Calculated time-averaged current $\langle I \rangle$ vs dc bias voltage V for a 10×10 homogeneous voltage-biased array at two values of f at $T = 0$. Other parameters as in Fig. 1. The curves are offset horizontally by 1.5 units. Insets: array resistance $\mathcal{R} \equiv V / \langle I \rangle$ (in unit of R) vs bias voltage V .

teristic it follows. Now consider a homogeneous current-biased array of such junctions. If the applied current is smaller than those of the individual junctions, then Eqs. (5)–(7) can all be satisfied with zero voltage through each junction. While these equations would also be satisfied if one or several rows switched into a resistive state, evidently this switching is not stabilized for current-biased homogeneous arrays, unless *all* the rows switch into a resistive state. On the other hand, if a homogeneous array is *voltage biased*, then in the range $0 < \langle V \rangle < NRI_c$ the differential equations *cannot* be satisfied if *all* the rows switch. Hence, in effect, the voltage bias is a boundary condition which forces individual row switching to occur. By contrast, when a homogeneous array is current biased, such row switching is not forced by the boundary conditions, and hence, need not occur (although we do not understand why it *never* seems to occur under current-biased conditions). Similarly, for an inhomogeneous current-biased array, there is a range of applied currents which exceeds the average critical current of some rows but not others. In that range of currents, it is reasonable that some rows should switch into a resistive state but not others. Since the individual shunt resistances in such arrays are unequal, we expect unevenly spaced resistance steps under such circumstances, as we find numerically.

To shed further light on the resistance steps, we have studied the time-averaged voltage of each grain and find that, for any given dc bias voltage V , each grain on a given row (such as the i th row) has the same time-averaged voltage V_i at any value of f . As V is increased, we find discontinuous jumps in each V_i , clearly revealing the row-switching behavior of the array. When $f = 0$, for our particular choice of (random) initial phases, the 8th step of Fig. 3 results from the simultaneous switching of two rows; hence, the total number of steps in this case is one fewer than the number of rows. We have also carried out simulations for larger arrays, and obtained similar results, including the occasional simultaneous switching of two or more rows.

In general, it is difficult to predict the exact number of steps, except to know that it cannot exceed the number of rows. The number of steps appears to depend on many factors, including the physical parameters of the array (β_c, β_d, R, I_c), the frustration f , the temperature T , and the initial conditions of the calculation. When there is no magnetic field, each jump occurs at an integer multiple of RI_c , but this need not be true at nonzero f , or in inhomogeneous arrays. It is also difficult to predict in the simulations which row will switch first in homogeneous arrays. This order also seems to depend on the same unpredictable factors which apparently determine the total number of steps. In a physical array, which can never be perfectly ordered, the switching presumably occurs first at the weakest part of the array, that is, the portion where the critical current of the junction is the lowest. Our simulations for inhomogeneous underdamped arrays confirm this prediction.

At finite temperatures, the behavior of the array can be understood in terms of thermally generated vortices. At low temperatures, these vortices are localized in

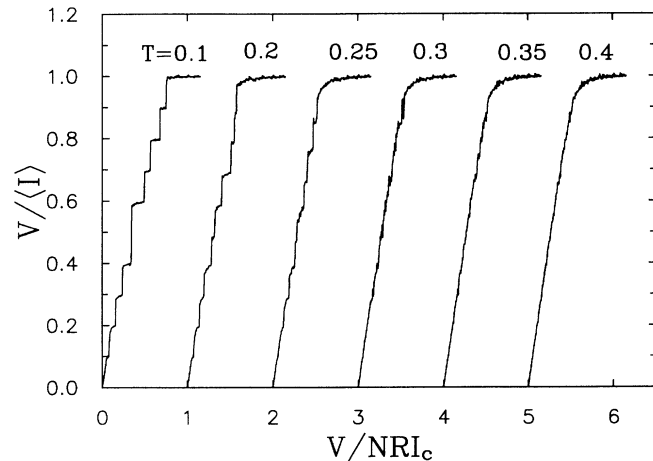


FIG. 4. Calculated time-averaged resistance $\mathcal{R} \equiv V/\langle I \rangle$ (in units of R) vs dc bias voltage V for a 10×10 homogeneous array at $f = 0$ and several values of temperature T [shown in units of $\hbar I_c/(2ek_B)$]. Other parameters as in Fig. 1. The curves are offset horizontally by one unit.

a two-dimensional periodic potential (the “egg-carton” potential^{27,28}) and the corresponding voltage is zero. At higher temperatures, a vortex can be thermally activated from one well to another of the egg-carton potential. The thermal activation tends to wash out and finally to melt the resistance steps. This can be seen in Fig. 4, which shows the results of a finite-temperature simulation on a 10×10 array at $f = 0$, using the same parameters as in Fig. 3. The melting temperature appears to be about $0.3\hbar I_c/(2ek_B)$, substantially below the expected Kosterlitz-Thouless transition temperature of about $0.95\hbar I_c(T_c)/(2ek_B)$,²⁹ presumably because our calculations are carried out at finite currents and voltages.

In order to investigate the relation between the resistance steps and the McCumber-Stewart parameters of

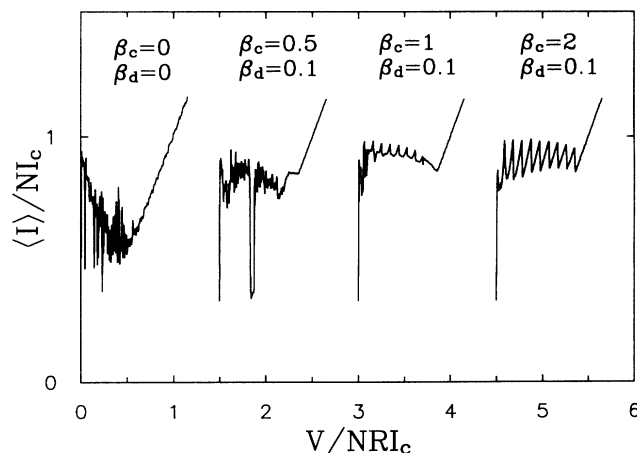


FIG. 5. Calculated time-averaged current $\langle I \rangle$ vs dc bias voltage V for a 10×10 homogeneous array at several values of the intergrain McCumber-Stewart parameter β_c at $f = 0$ and $T = 0$. The curves are offset horizontally by 1.5 units.

the array, we have also carried out simulations for different values of β_c . Our results are shown in Fig. 5, which corresponds to a voltage-driven homogeneous array at $T = 0$ and $f = 0$. The row-switching behavior evidently becomes weaker and weaker as β_c is reduced. In the overdamped limit ($\beta_c = \beta_d = 0$), there is no evidence at all for row-switching behavior. We conclude tentatively that the observed row-switching behavior, and corresponding resistance steps, are characteristics of underdamped arrays only.

The β_c dependence of Fig. 5 is physically reasonable. In an individual *underdamped* junction, as noted earlier, the resistance $\langle V \rangle / I$ is nearly bimodal at sufficiently large β_c (i.e., equal to either 0 or R on the two branches). By contrast, in an overdamped junction, $\langle V \rangle$, and hence $\langle V \rangle / I$, increase smoothly with I for $I > I_c$. Since individual overdamped junctions thus do not have resistance plateaus, we would not expect such plateaus in arrays either.

To summarize, we have numerically studied the re-

sponse of underdamped Josephson-junction arrays to an applied dc bias current and dc bias voltage. The resulting $I - V$ curves exhibit substantial hysteresis. Current-biased inhomogeneous arrays display many steps on a plot of resistance versus current. These steps result from the simultaneous switching of one or several rows across the width of the array from a supercurrent state to a resistively dissipative state. In voltage-biased arrays, this row-switching behavior is found even in homogeneous arrays. The numerical simulations reveal that these steps persist in an applied magnetic field and at finite temperatures. There is no evidence for row switching or resistance steps in overdamped arrays. Our calculations are generally consistent with experiments.

This work was supported by National Science Foundation through Grant No. DMR 90-20994. Calculations were carried out, in part, on the CRAY Y-MP8/864 of the Ohio Supercomputer Center. Valuable conversations with Dr. K. H. Lee are gratefully acknowledged.

- ¹S. P. Benz, M. S. Rzchowski, M. Tinkham, and C. J. Lobb, Phys. Rev. Lett. **64**, 693 (1990); Physica **B165-66**, 1645 (1990).
²H. C. Lee, D. B. Mast, R. S. Newrock, L. Bortner, K. Brown, F. P. Esposito, D. C. Harris, and J. C. Garland, Physica **B165-66**, 1571 (1990).
³K. H. Lee, D. Stroud, and J. S. Chung, Phys. Rev. Lett. **64**, 962 (1990); J. S. Chung, K. H. Lee, and D. Stroud, Phys. Rev. B **40**, 6570 (1989).
⁴J. U. Free, S. P. Benz, M. S. Rzchowski, M. Tinkham, C. J. Lobb, and M. Octavio, Phys. Rev. B **41**, 7267 (1990).
⁵T. C. Halsey, Phys. Rev. B **41**, 11 634 (1990); S. J. Lee and T. C. Halsey (unpublished).
⁶K. H. Lee and D. Stroud, Phys. Rev. B **43**, 5280 (1991).
⁷M. Octavio, J. U. Free, S. P. Benz, R. S. Newrock, D. B. Mast, and C. J. Lobb, Phys. Rev. B **44**, 4601 (1991).
⁸Wenbin Yu, E. B. Harris, S. E. Hebboul, J. C. Garland, and D. Stroud, Phys. Rev. B **45**, 12 624 (1992).
⁹W. Xia and P. L. Leath, Phys. Rev. Lett. **63**, 1428 (1989).
¹⁰K. K. Mon and S. Teitel, Phys. Rev. Lett. **62**, 673 (1989).
¹¹A. Falo, A. R. Bishop, and P. S. Lomdahl, Phys. Rev. B **41**, 10 983 (1990); N. Grønbech-Jensen, A. R. Bishop, F. Falo, and P. S. Lomdahl, Phys. Rev. B **45**, 10 139 (1992); **46**, 11 149 (1992).
¹²H. Eikmans and J. E. Van Himbergen, Phys. Rev. B **41**, 8927 (1990).
¹³L. I. Sohn, M. S. Rzchowski, J. U. Free, S. P. Benz, M. Tinkham, and C. J. Lobb, Phys. Rev. B **44**, 925 (1991).
¹⁴D. Domínguez, J. V. José, A. Karma, and C. Wiecko, Phys. Rev. Lett. **67**, 2367 (1991).
¹⁵S. R. Shenoy, J. Phys. C **18**, 5163 (1985).
¹⁶R. Bhagavatula, C. Ebner, and C. Jayaprakash, Phys. Rev. B **45**, 4774 (1992).

- ¹⁷For additional references to work prior to 1989, see the articles in Physica **152B+C** (1988), and references cited therein.
¹⁸H. S. J. van der Zant, C. J. Muller, L. J. Geerligs, C. J. P. M. Harmans, and J. E. Mooij, Phys. Rev. B **38**, 5154 (1988).
¹⁹T. S. Tighe, A. T. Johnson, and M. Tinkham, Phys. Rev. B **44**, 10 286 (1991).
²⁰H. S. J. van der Zant, F. C. Fritschy, T. P. Orlando, and J. E. Mooij, Physica **B165-66**, 969 (1990).
²¹H. S. J. van der Zant, F. C. Fritschy, T. P. Orlando, and J. E. Mooij, Phys. Rev. Lett. **66**, 2531 (1991).
²²V. Ambegaokar and B. I. Halperin, Phys. Rev. Lett. **22**, 1364 (1969).
²³W. C. Stewart, Appl. Phys. Lett. **22**, 277 (1968); D. E. McCumber, J. Appl. Phys. **39**, 3113 (1968).
²⁴Rosario Fazio and Gerd Schön, Phys. Rev. B **43**, 5307 (1991).
²⁵M. S. Rzchowski, S. P. Benz, M. Tinkham, and C. J. Lobb, Phys. Rev. B **42**, 2041 (1990).
²⁶V. Ambegaokar and A. Baratoff, Phys. Rev. Lett. **10**, 486 (1963); **11**, 104(E) (1963).
²⁷C. J. Lobb, D. W. Abraham, and M. Tinkham, Phys. Rev. B **27**, 150 (1983).
²⁸K. H. Lee, D. Stroud, and J. S. Chung, in *Proceedings of the NATO Advanced Research Workshop on Relaxation in Complex Systems and Related Topics*, edited by I. A. Campbell and C. Giovannella (Plenum, New York, 1990), pp. 123-130.
²⁹J. M. Kosterlitz and D. J. Thouless, J. Phys. C **6**, 1181 (1973); S. Teitel and C. Jayaprakash, Phys. Rev. B **27**, 598 (1983).